




The potential use of tideglusib as an adjuvant radio-therapeutic treatment for glioblastoma multiforme cancer stem-like cells

Jolie Bou-Gharios^{1,2} · Sahar Assi¹ · Hisham F. Bahmad^{1,3} · Hussein Kharroubi¹ · Tarek Araji¹ · Reda M. Chalhoub^{1,4} · Farah Ballout¹ · Hayat Harati² · Youssef Fares² · Wassim Abou-Kheir¹ 

Received: 4 July 2020 / Revised: 17 October 2020 / Accepted: 20 October 2020 / Published online: 2 November 2020
© Maj Institute of Pharmacology Polish Academy of Sciences 2020, corrected publication 2020

Abstract

Background Glioblastoma multiforme (GBM), a stage IV astrocytoma, is the most common brain malignancy among adults. Conventional treatments of surgical resection followed by radio and/or chemotherapy fail to completely eradicate the tumor. Resistance to the currently available therapies is mainly attributed to a subpopulation of cancer stem cells (CSCs) present within the tumor bulk that self-renew leading to tumor relapse with time. Therefore, identification of characteristic markers specific to these cells is crucial for the development of targeted therapies. Glycogen synthase kinase 3 (GSK-3), a serine–threonine kinase, is deregulated in a wide range of diseases, including cancer. In GBM, GSK-3 β is overexpressed and its suppression *in vitro* has been shown to induce apoptosis of cancer cells.

Methods In our study, we assessed the effect of GSK-3 β inhibition with Tideglusib (TDG), an irreversible non-ATP competitive inhibitor, using two human GBM cell lines, U-251 MG and U-118 MG. In addition, we combined TDG with radiotherapy to assess whether this inhibition enhances the effect of standard treatment.

Results Our results showed that TDG significantly reduced cell proliferation, cell viability, and migration of both GBM cell lines in a dose- and time-dependent manner *in vitro*. Treatment with TDG alone and in combination with radiation significantly decreased the colony formation of U-251 MG cells and the sphere formation of both cell lines, by targeting and reducing their glioblastoma cancer stem-like cells (GSCs) population. Finally, cells treated with TDG showed an increased level of unrepaired radio-induced DNA damage and, thus, became sensitized toward radiation.

Conclusions In conclusion, TDG has proven its effectiveness in targeting the cancerous properties of GBM *in vitro* and may, hence, serve as a potential adjuvant radio-therapeutic agent to better target this deadly tumor.

Keywords Glioblastoma multiforme · Tideglusib · GSK-3 β · Radiation · Cancer stem cells · Glioblastoma stem-like cells · Sphere-formation assay

Jolie Bou-Gharios, Sahar Assi and Hisham F. Bahmad have contributed equally to this work as co-first authors.

Youssef Fares and Wassim Abou-Kheir have contributed equally to this work as joint senior authors.

Electronic supplementary material The online version of this article (<https://doi.org/10.1007/s43440-020-00180-5>) contains supplementary material, which is available to authorized users.

✉ Youssef Fares
yfares@ul.edu.lb

✉ Wassim Abou-Kheir
wa12@aub.edu.lb

Extended author information available on the last page of the article

Introduction

Glioblastoma Multiforme (GBM), grade IV astrocytoma, is the most common central nervous system (CNS) tumor in adults, accounting for 45.6% of primary malignant brain tumors [1, 2]. It is an invasive and highly aggressive cancer that is rapidly fatal with an average median survival of one year after diagnosis [3]. Current treatments include surgical resection as a mainstay; however, the tumor is barely entirely removed due to the surrounding infiltrating cells which evade the normal tissue and are hard to be distinguished from one another [4]. Therefore, surgical processes are often followed by radiotherapy up to 46 Gy divided over 23 fractions, i.e., 2 Gy per fraction [5] and/or chemotherapy mainly Temozolomide (TMZ) [3, 6,

7]. Recently, studies have shown that TMZ—when combined with radiotherapy—can significantly improve the median survival of GBM patients [8, 9]. However, there has been only minor improvements in the prognosis of GBM patients due to an intrinsic tendency of the tumor to develop radiotherapy and chemotherapy resistance [7, 10].

Despite advances in research, conventional treatment regimens have failed to completely eradicate the tumor due to the presence of a cancer stem cell (CSC) subpopulation within the heterogeneous bulk of this tumor, leading to recurrence and progression to a more aggressive form [11–13]. Molecular analyses of GBM stem cells, known as glioblastoma cancer stem-like cells (GSCs) [14], revealed several genetic lesions and altered pathways that are implicated in tumor pathogenesis, characterizing this aggressive tumor. This has paved the way for investigating novel therapies that are targeted against this cell subpopulation, in an attempt to eradicate the tumor and prevent its recurrence [12, 15–17].

Among these molecular markers is glycogen synthase kinase 3 beta (GSK-3 β), a serine/threonine protein kinase that plays a crucial role in the regulation of several cellular pathways through its interaction with a wide array of substrates, influencing cell structure, motility, and survival [18]. The complexity of its effects explains the pivotal role of its dysregulation in the pathogenesis of many diseases. It has been proven to act as a promoter of inflammation, playing a key role in the development of several chronic pathologies including CNS diseases such as Alzheimer's disease [18, 19]. In cancer, the role of GSK-3 β is still debatable since it may act as a tumor promoter or a tumor repressor depending on the type of cancer involved. In the case of GBM, the expression and activity of GSK-3 β has been shown to be deregulated and its inhibition was shown not only to affect tumor cell proliferation and survival, but also to enhance its susceptibility to both ionizing radiation and chemotherapeutic agents [7] and induce cellular apoptosis as well [20]. Therefore, inhibiting GSK-3 β might represent a potential therapeutic strategy to target GBM.

Interestingly, Tideglusib, a GSK-3 β inhibitor, has been investigated in phase II clinical trials for Alzheimer's disease and progressive supranuclear palsy [21, 22] and was proven to be safe and well tolerated [23]. Unlike other GSK-3 β inhibitors, TDG is a non-ATP competitive inhibitor, a property that allows it to have better selectivity for GSK-3 β on one hand and a lower IC₅₀ value on the other hand, avoiding cytotoxicity [24]. A study showed that TDG specifically inhibits GSK-3 β irreversibly and follows a specific inhibitory mechanism linked to the presence of Cys-199 [25]. Its effect on different cancer types has also been investigated in vitro, such as in neuroblastoma [26], ovarian teratocarcinoma [27], and prostate cancer [28].

Based on what is mentioned above, we decided to investigate the potential use of TDG in the treatment of GBM by assessing its effect on two human GBM cell lines U-251 MG and U-118 MG. In addition, since combinatorial treatments have been shown to be efficacious in the treatment of GBM, we wanted to investigate the effect of combining TDG with radiotherapy, the first line of treatment in GBM after surgery, and to assess the capacity of this combination to better target the cancerous properties of GBM in vitro, in 2D and 3D culture systems (Fig. 1). Therefore, the purpose of this study was to introduce TDG as a novel therapeutic approach to treat GBM and to inspect whether this drug might ameliorate the effect of radiation, in an attempt to improve the quality of life of GBM patients.

Materials and methods

Cell culture and treatment

U-251 MG (ECACC® 09,063,001; RRID:CVCL_0021) [29] and U-118 MG (ATCC® HTB-15™, USA; RRID:CVCL_0633) [29, 30] cells were cultured and maintained in Dulbecco's Modified Eagle Media (DMEM) Ham's F-12 (Sigma-Aldrich; cat #D8437) supplemented with 10% heat inactivated fetal bovine serum (FBS) (Sigma-Aldrich; cat #F9665), 1% Penicillin/Streptomycin (Biowest; cat #L0022-100), and 0.2% Plasmocin™ prophylactic (InvivoGen; cat #ant-mpp). Cells were incubated at 37 °C in a humidified incubator containing 5% CO₂. The drug Tideglusib (TDG) was purchased from Sigma-Aldrich (cat #SML0339-10MG; Lot # 123M4615V and 016M4605V) and was reconstituted in 0.1% dimethyl sulfoxide (DMSO; Amresco; cat #0231-500ML), per manufacturer's instructions.

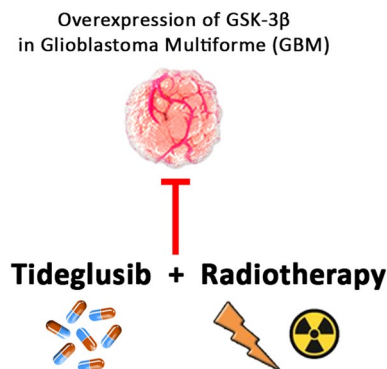


Fig. 1 Schematic illustration showing the combinatorial effect of tideglusib and radiotherapy and its capacity in inhibiting GSK-3 β overexpression in glioblastoma multiforme (GBM)

Irradiation

Cells were radiated with a 225-kV Precision X-Ray (PXi) irradiator model No X-RAD 225. Radiation was performed at $3 \text{ Gy}\cdot\text{min}^{-1}$ and a 1.5-mm Aluminum filter was used. All cells were radiated at a dose of 2 Gy equivalent to the dose given to patients per radiotherapy session in clinics.

MTT/Cell viability assay

The anti-proliferative effect of TDG was measured in vitro using MTT ([3-(4, 5-dimethylthiazol-2-yl)-2, 5-diphenyltetrazolium bromide]) (Sigma-Aldrich; cat #M5655-1G) assay according to the manufacturer's instructions [31–33]. Briefly, U-251 MG and U-118 MG cells were seeded (2×10^3 cells/well) in 100- μL complete growth medium in 96-well plates and incubated overnight at 37°C , 5% CO_2 . Cells were treated with different concentrations of TDG (5 μM , 25 μM , or 50 μM) for 24, 48 and 72 h. At each time point, media was removed and replaced with fresh media along with 10 μL /well of the MTT yellow dye (5 mg/mL in DMSO) and incubated for 4 h, after which 100 μL of the solubilizing agent was added to each well and left overnight. The absorbance intensity was measured by the microplate ELISA reader (Multiscan EX) at a wavelength of 595 nm. The percentage of cell proliferation was presented as an optical density (OD) ratio of the treated to the untreated cells. Two-way ANOVA, followed by Bonferroni multiple comparisons test, was done to compare the means of the different conditions to that of the control group within the three different time points.

Trypan Blue/Cell exclusion assay

The effect of TDG on cell viability was measured in vitro using trypan blue assay [34]. U-251 MG and U-118 MG cells were cultured in 24-well plates (2×10^4 cells/well) and incubated at 37°C , 5% CO_2 . After reaching 60–70% confluency, cells were treated with different concentrations of TDG (5 μM , 25 μM or 50 μM) for 24, 48 and 72 h. At each time point, cells were trypsinized and viable ones were counted using a hemocytometer under an inverted light microscope after staining cell suspensions with Trypan blue. The percentage of cell viability was presented as a ratio of viable cells counted in treated to untreated conditions. Two-way ANOVA, followed by Bonferroni multiple comparisons test, was done to compare the means of the different conditions to that of the control group within the three different time points.

Wound healing assay

The effect of TDG on cell migration was assessed in vitro using wound healing assay. U-251 MG and U-118 MG cells were cultured in 12-well plates (10^5 cells/well) and incubated at 37°C , 5% CO_2 . After reaching 80–90% confluency, cells were treated with 10 mg/mL of Mitomycin C (Sigma-Aldrich; cat #M0503-5 \times 2MG) for 1 h to inhibit cellular proliferation, after which two uniform scratches of similar width were made using a sterile 200- μL micropipette tip. Prior to the addition of TDG to the treatment conditions, cells were washed twice with PBS to remove Mitomycin C and thus, no direct effect was present between TDG and Mitomycin C. In fact, the main purpose behind using Mitomycin C is to inhibit cellular proliferation while maintaining the migration potential of cancer cells. Plates were then washed twice with Dulbecco's phosphate-buffered saline (D-PBS) (Sigma-Aldrich; cat #D8537-500ML) to eliminate the detached cells. The remaining cells were cultured in complete growth media as control (untreated) or treated with 25 μM of TDG. Bright-field images were taken at different time points (0, 6, 18, 24 and 48 h) until the wounds closed completely in the untreated group (control). The distance of the wound was measured using Zen Software (Zen 2.3) and the distance traveled by the cells enumerated the closure of the wounds. Two-way ANOVA was performed followed by Bonferroni multiple comparisons test to compare the mean of the treated conditions to that of the control and within the different time points chosen.

Cell survival/clonogenic assay

The effect of TDG and irradiation on the colony-forming ability of the cells was assessed in vitro using the clonogenic assay. Cells were cultured in 6-well plates and incubated at 37°C , 5% CO_2 . Upon reaching 70% confluency, clonogenic assay with the delayed plating technique was performed: cells were either irradiated with a dose of 2 Gy or treated with different doses of TDG (5 μM and 25 μM) and incubated for 24 h; while, others were treated with TDG for 24 h then irradiated with a dose of 2 Gy and incubated for another 24 h. After the period of incubation, cells were re-seeded in 6-well plates at two different concentrations (1×10^3 and 2×10^3 cells/well) which were chosen based on the best plating efficiency of each cell line. After an incubation period of 7 days, cells were fixed with 95% ethanol, washed with PBS, stained with crystal violet, and washed with distilled water. Stained colonies with more than 50 cells each were counted [35]. Surviving fraction (SF) was presented as a percentage of counted colonies in treated conditions to number of counted colonies in control group. One-way ANOVA followed by a Bonferroni multiple comparisons test was done to compare the means of the treated conditions (TDG or

TDG + RT) to that of the control, and a parametric unpaired t-test was done to compare the mean of RT-treated condition with that of the control.

Immunofluorescence

Cells were grown in 24-well plates on 12-mm glass coverslips placed at the bottom of each well (2×10^4 /well). After incubation, cells were either irradiated with a dose of 2 Gy and fixed at specific time points, treated with TDG for 24 h and then fixed, or treated with TDG for 24 h followed by irradiation of 2 Gy and then fixed. The time points for fixation were at 10 min and 24 h post-irradiation. Cells were fixed with 4% paraformaldehyde for 15 min at room temperature and permeabilized using 0.1% Triton X-100 solution for 3 min at 4 °C. After fixation, immunofluorescence assay was performed. Cells were first incubated with Anti- γ H2AX (ser139) antibody (dilution 1:500) (Millipore; cat #05,636) for 1 h at 37 °C, then with goat anti-mouse secondary antibody (Alexa Fluor 488 goat anti-mouse IgG) (dilution 1:100) for 20 min at 37 °C. Then, the coverslips were mounted using Fluoroshield Mounting Medium with DAPI (4',6'-Diamidino-2-Phenyl-indole) (Abcam; cat #ab104139) and examined with Zeiss LSM 710 confocal fluorescent microscope. Two-way ANOVA followed by Bonferroni multiple comparisons test was done to compare the mean of all conditions within one another at the three given time points. In addition, a one-way ANOVA was performed to compare the means of treated conditions at a single time point (24 h), followed by Bonferroni multiple comparisons test.

Western blotting analysis

U-251 MG and U-118 MG cells were cultured in T25 flasks and incubated at 37 °C, 5% CO₂ until they reached 70% confluence. Flasks were randomly assigned as control (untreated) and treated with a concentration of 25 μ M of TDG for 24 h. The plates were then washed with PBS to remove any residual media. Adherent cells were treated with radioimmunoprecipitation (RIPA) buffer (0.1% sodium dodecyl sulfate (SDS) (v/v), 0.5% sodium deoxyolate (v/v), 150 mM sodium chloride (NaCl), 100 mM EDTA, 50 mM Tris-HCl (pH=8), 1% Tergitol (NP40) (v/v), 1 mM PMSF, and protease and phosphatase inhibitors (one tablet of each in 10 mL buffer, Roche, Germany)), scraped off the plates, transferred into micro-centrifuge tubes and incubated on ice for 30 min. Sonication was used to maximize the protein yield. Lysates were then centrifuged at 13,600 rpm for 20 min at 4 °C, to pellet the cell debris.

Protein quantification was performed using DC™ Protein Assay (Bio-Rad) as per the manufacturer's recommendations, with serial dilutions of bovine serum albumin (BSA) (v/v) (Amresco; cat #0332-100G) taken as standards.

Aliquots of proteins of equal amounts (50 μ g) were mixed with sample buffer (with 5% β -mercaptoethanol) and separated on 12% SDS-PAGE gel. Proteins were transferred into PVDF membranes (Bio-Rad Laboratory, CA, USA) for 2 h, and were later blocked using 5% milk in Tris-buffered Saline (TBS) with 0.1% Tween-20. The blots were incubated overnight at 4 °C with specific mouse primary antibodies in TBS with 5% BSA, targeting: phosphorylated GSK-3 β (Ser9) (1:500 dilution; Cell Signaling Technology; cat #9323), total GSK-3 β (1:1000 dilution; Cell Signaling Technology; cat #27C10) and GAPDH (1:5000 dilution; Novus Biologicals; cat #NB300-221) as a loading control. Then, membranes were incubated at room temperature for 2 with HRP-conjugated secondary antibodies as follows: mouse anti-rabbit (1:1000 dilution; Santa Cruz; cat #sc-2357) and mouse IgGk BP (1:1000 dilution; Santa Cruz; cat #sc-516102). Bands were then detected by enhanced chemiluminescence (ECL) using ChemiDoc MP Imaging System (BioRad) and were analyzed using ImageJ software (RRID:SCR_003070). A parametric unpaired t-test was done to each cell line separately to compare the mean of treated group to that of the control.

3D culture and sphere-formation assay

U-251 MG and U-118 MG cells were cultured in growth factor-reduced (GFR) Matrigel™/serum-free DMEM F-12 Ham (1:1) at a concentration of 4×10^3 cells/well in a total volume of 50 μ l. The solution was plated gently around the bottom rim of individual wells of 24-well plates in a uniform circular manner and Matrigel™ (Corning Life Sciences; cat #354,230) was allowed to solidify for 1 h at 37 °C, 5% CO₂. Next, cells plated in Matrigel™ were either radiated with a dose of 2 Gy, treated with TDG (0.1 μ M, 1 μ M, or 5 μ M), or irradiated (2 Gy) and treated with TDG (0.1 μ M or 1 μ M). The media were gently added to the center of each well and consisted of 0.5 mL of DMEM with 5% FBS per well, with or without treatment, and were replenished every 2–3 days. Spheres were counted at day 7 after plating (U-118 MG) or at day 9 (U-251 MG) and the sphere-forming unit (SFU) was calculated as a percentage of the number of spheres counted to the number of input cells. Carl Zeiss Zen 2012 image software was then used to analyze sphere images to quantify the average size of U-251 MG and U-118 MG spheres with or without the different treatments. Data represent the average area (μ m²) of spheres from three independent experiments, where average size of 30 spheres per condition per experiment was considered. One-way ANOVA was done to compare the means of the treated conditions (TDG or TDG + RT) to that of the control, and a parametric unpaired t-test was done to compare the mean of RT-treated condition with that of the control.

Data analyses

Statistical analysis was performed using GraphPad Prism 7 Software. Data presented are the means \pm SEM of three separate experiments. The significance of the data was analyzed using a simple t-test, one-way ANOVA and two-way ANOVA statistical tests, followed by multiple comparisons test using Bonferroni post hoc analysis. Statistical significance was reported when the p-value was less than 0.05 (* $p < 0.05$; ** $p < 0.01$; *** $p < 0.001$).

Results

Tideglusib reduces cell proliferation and viability of U-251 MG and U-118 MG cell lines

The in vitro effect of increasing concentrations of TDG on cell proliferation and cell viability of human GBM cell lines, U-251 MG and U-118 MG, was assessed using MTT assay (Fig. 2a and b) and trypan blue exclusion assay (Fig. 2c and d), respectively. TDG significantly inhibited the proliferative ability and cell viability of both cell lines in a time- and dose-dependent manner. After 48 h of treatment with 25 μ M TDG, cell proliferation was inhibited by approximately

50% for U-251 MG and 60% for U-118 MG ($p = 1.1 \times 10^{-7}$; $F_{8,30} = 9.58$). Similarly, the cellular viability of U-251 MG significantly decreased by 50% after 24 h of treatment with 5- μ M TDG ($p = 6.0413E-06$; $F_{8,30} = 0.95$). As for U-118 MG, the viability decreased significantly by 50% after 48 h of treatment with 25- μ M TDG ($p = 0.00036$; $F_{8,30} = 0.65$). We decided to proceed the following experiments with either 5- μ M or 25- μ M TDG based on two main reasons: (1) almost half of the cells were dead at this concentration either at 24 h or at 48 h post-treatment, and (2) at very high concentrations of TDG, crystals of this drug were formed and were suspected to affect the environment surrounding the cells; thus, we refrained from the use of such high concentrations to limit the external factors directly affecting the cells.

Tideglusib inhibits the migratory ability of U-251 MG and U-118 MG cell lines

We next investigated the effect of TDG on the migration ability of both cell lines using a scratch/wound healing assay in which the cells were either left untreated (control) or treated with 25 μ M of TDG. Cells were treated with Mitomycin C to inhibit cellular proliferation prior to wound formation (Fig. 3a). Results revealed that while the wound almost completely healed in the untreated group after 48

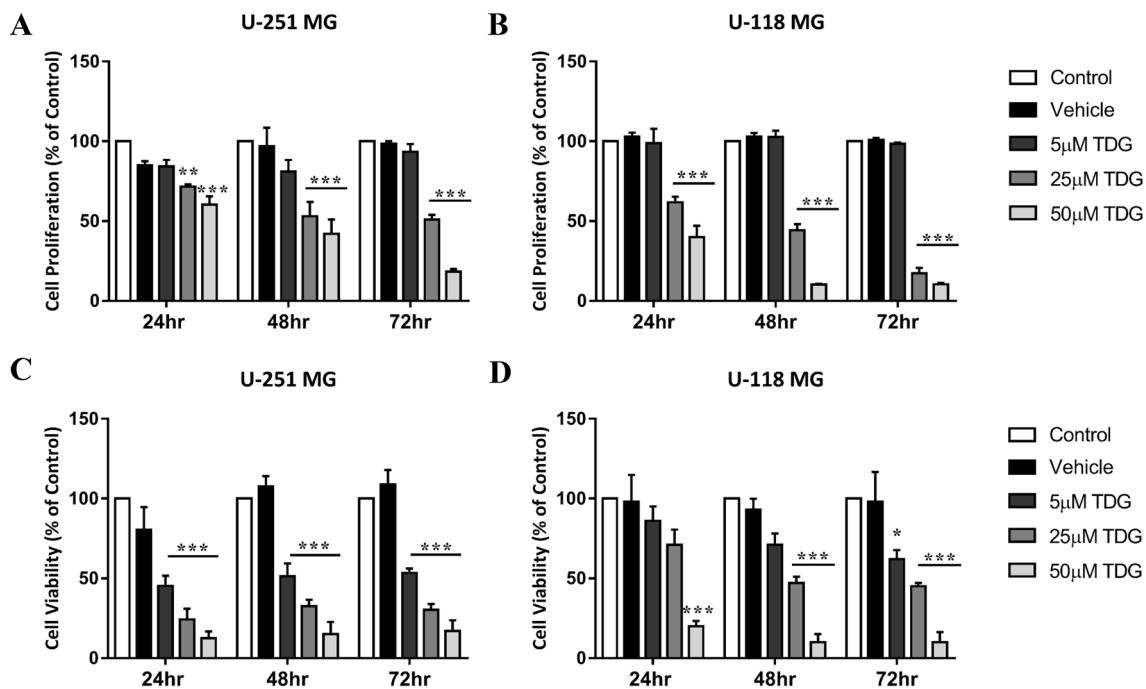


Fig. 2 Tideglusib reduces cell proliferation and viability of human glioblastoma cell lines in a time- and dose-dependent manner in vitro. After incubation of the two cell lines U-251 MG and U-118 MG for 24, 48, and 72 h with or without TDG, cell proliferation was determined using the MTT assay (a, b). Cell viability was assessed using the trypan blue exclusion assay; cells were treated with increasing

doses of TDG for 24, 48, and 72 h (c, d). Two-way ANOVA was done followed by a Bonferroni multiple comparisons test. Results are expressed as a percentage of treated versus the control group. Data represent an average of three independent experiments and are expressed as mean \pm SEM (error bars). (* $p < 0.05$; ** $p < 0.01$; *** $p < 0.001$)

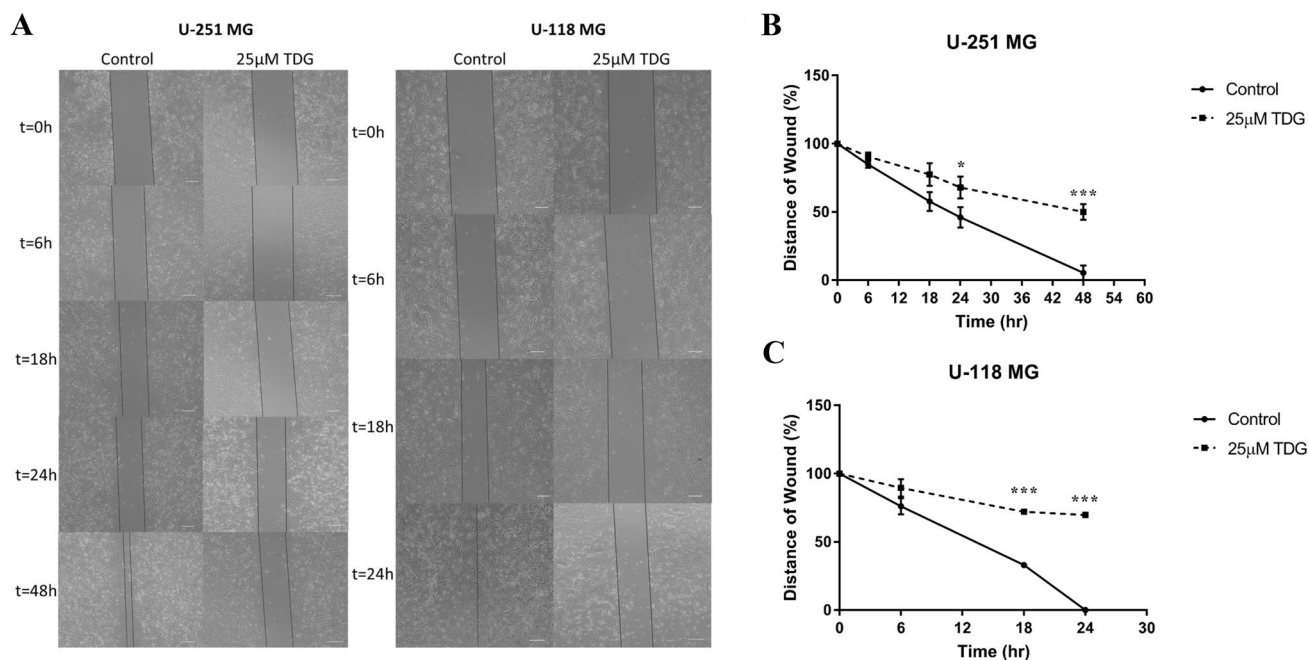


Fig. 3 Tideglusib reduces the migratory potentials of human glioblastoma cell lines in vitro. **a** Representative bright-field images showing the effect of 25- μ M TDG on cell migration. Images of the scratch made were taken at T=0, 6, 18, 24 and 48 h post-wound formation in the control wells (without TDG) and in the treated wells. The cancerous property of migration was assessed by quantifying the wound closure over time. Magnification = 5x; Scale bar = 200 μ m. The wound in untreated cells closed at 48 h and 24 h for U-251 MG and U-118 MG,

respectively, while TDG was able to significantly inhibit the migration of both cell lines at different time points. At 48 h post-treatment, TDG halted cell migration of U-251 MG by 45% (**b**) and by almost 70% for U-118 MG (**c**). Two-way ANOVA was done followed by Bonferroni multiple comparisons test. Results are expressed as a percentage of treated versus the control group at different time points. Data represent an average of three independent experiments and are expressed as mean \pm SEM. (* p < 0.05; *** p < 0.001)

and 24 h in U-251 MG and U-118 MG cell lines, respectively, TDG significantly suppressed wound closure in the treated conditions by almost 50% in U-251 MG and 70% in U-118 MG (Fig. 3b and c) (p = 6.99129E-06; $F_{8,30}$ = 3.14 and p = 10^{-12} ; $F_{9,32}$ = 17.55, respectively), suggesting an inhibition of the cells' migratory abilities by the drug.

Tideglusib inhibits GSK-3 β

The direct effect of Tideglusib on its target GSK-3 β was assessed using western blot by detecting the differences in protein expression between the treated and untreated lysates. TDG was able to increase the protein expression of p-GSK-3 β (ser9), the inhibited form of GSK-3 β to 3.92 (p = 0.0123; t = 4.3392; DF = 4) and 1.29 (p = 0.27; t = 1.2791; DF = 4) for U-251 MG and U-118 MG, respectively (Fig. 4a and b; Supplementary Figure S1 and S2).

The combination of Tideglusib and radiation reduces the colony formation of U-251 MG cell line

Clonogenic assay was performed on U-251 MG cell line only since U-118 MG cells were unable to form colonies. A low dose of 5- μ M TDG was able to reduce the surviving

fraction of U-251 MG by 10% (p = 0.120461367; $F_{2,6}$ = 2.3), while a higher dose of 25 μ M significantly reduced the colony formation by 60% (p = 3.37033E-05; $F_{2,6}$ = 12.39248) (Fig. 5a). A single dose of 2 Gy, clinically applied per one session of radiotherapy, reduced the colony formation by 50% (p = 1.78771E-05; t = 24; DF = 4) (Fig. 5b). However, when combined, 25- μ M TDG + 2 Gy were able to significantly reduce the colony formation by 80% (p = 7.74E-08; $F_{2,6}$ = 34.61939) (Fig. 5c) displaying an additive effect between both treatments.

Tideglusib sensitizes U-251 MG and U-118 MG cell lines to X-ray radiation

Since the double-strand breaks are the most dangerous type of DNA damage caused by radiation, we decided to study the repair of DNA double-strand breaks (DSBs) using immunofluorescence by assessing the appearance and disappearance of γ H2AX foci at different time points after exposure of U-251 MG and U-118 MG cell lines to ionizing radiation (IR) alone or in combination with different concentrations of TDG (Fig. 6a and c). A single dose of 2 Gy induced 65 ± 3.9 foci in U-251 MG and 73 ± 7.3 in U-118 MG 10 min post-IR. Generally, the number of γ H2AX foci, detected 10 min post-IR, was

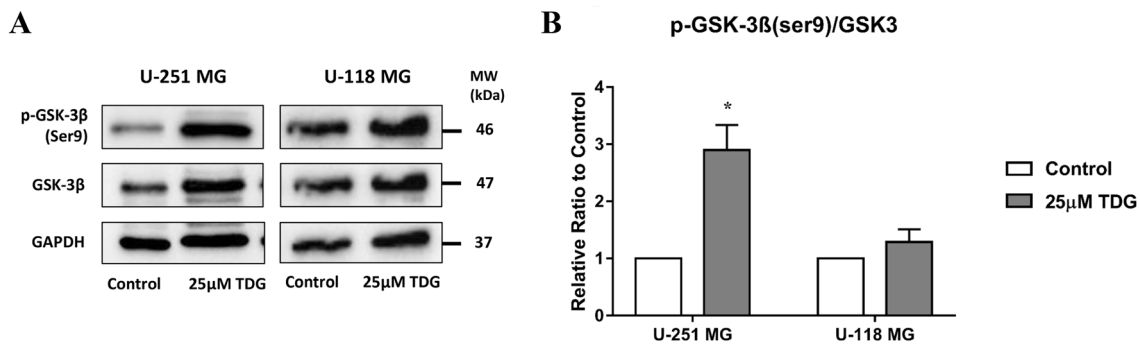


Fig. 4 Tideglusib selectively inhibits GSK-3 β by increasing expression of its inhibited form, phosphorylated at Serine 9 (p-GSK-3 β Ser 9). After treating cells with 25 μ M TDG, proteins were extracted using RIPA buffer, and used to detect differences in expression of the phosphorylated form of GSK-3 β (Ser 9). **a** Bands were detected by enhanced chemiluminescence (ECL) using ChemiDoc MP Imaging System. **b** Protein expression was quantified using ImageJ software,

relative to the expression of GAPDH, a housekeeping gene. Analysis of p-GSK-3 β (Ser 9) protein level was done after normalization with total GSK-3 β protein levels. A parametric unpaired t-test was done to compare means of treated versus untreated groups of each cell line. Results are expressed as relative ratio to control. Data represent an average of three independent experiments. The data are reported as mean \pm SEM (* p < 0.05)

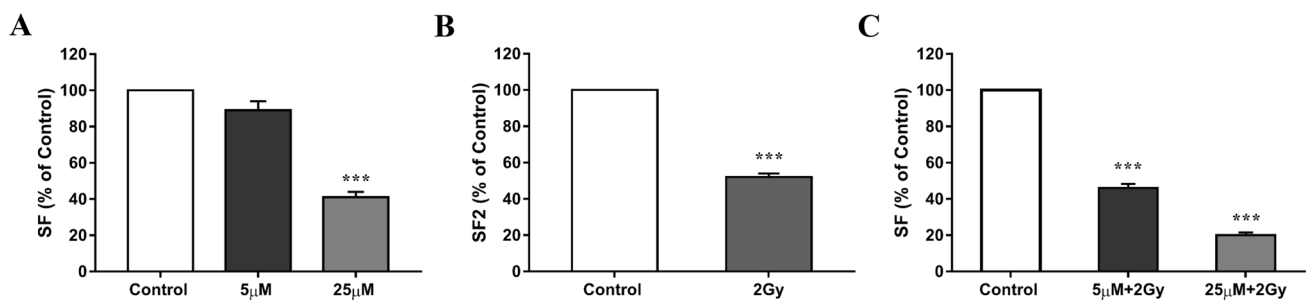


Fig. 5 Tideglusib when combined with RT decreases the colony formation of U-251 MG most efficiently. Clonogenic assay with the delayed plating technique was performed after 24 h of treatment with (i) TDG (5 μ M and 25 μ M) (**a**), (ii) radiation at a dose of 2 Gy (**b**) and (iii) the combination of TDG (5 μ M and 25 μ M) + RT (2 Gy) (**c**). The surviving fraction of cells treated with TDG or TDG + RT is referred to as SF, while that of cells treated with 2 Gy is referred to as

SF2. Results are expressed as the percentage of counted colonies in treated conditions/colonies counted in untreated group (control). One-way ANOVA (with Bonferroni post hoc) and *t*-test were done to analyze the different treatment conditions. Results are expressed as a percentage of treated versus the control group. Data represent an average of three independent experiments and are expressed as mean \pm SEM. (***) p < 0.001

significantly higher for all combinatorial treatments as compared to radiation alone (Fig. 6b and d) and was dose dependent in U-251 MG. On the other hand, the residual number of γ H2AX foci decreased significantly 24 h post-IR reaching 3 ± 0.5 ($p = 10^{-12}$; $F_{2,240} = 68.6937$) and 3.6 ± 1.6 ($p = 10^{-12}$; $F_{2,226} = 63.9193$) foci in U-251 MG and U-118 MG, respectively. However, when cells were treated with the combination of TDG + RT, a higher residual of γ H2AX foci number was reached as compared to the radio-induced γ H2AX foci 24 h post-radiation, indicating the potential of TDG in sensitizing GBM to radiation.

Tideglusib in combination with radiation therapy decreases the sphere-forming capacity and the size of U-251 MG and U-118 MG spheres

Sphere-formation assay was performed in which U-251 MG and U-118 MG cells were cultured in MatrigelTM for 9 and 7 days, respectively. The sphere-forming ability, and hence the cancer stem-like properties of GBM cell lines, was assessed in treated versus non-treated cells. The obtained spheres were visualized and counted using an inverted light microscope and images were taken using the

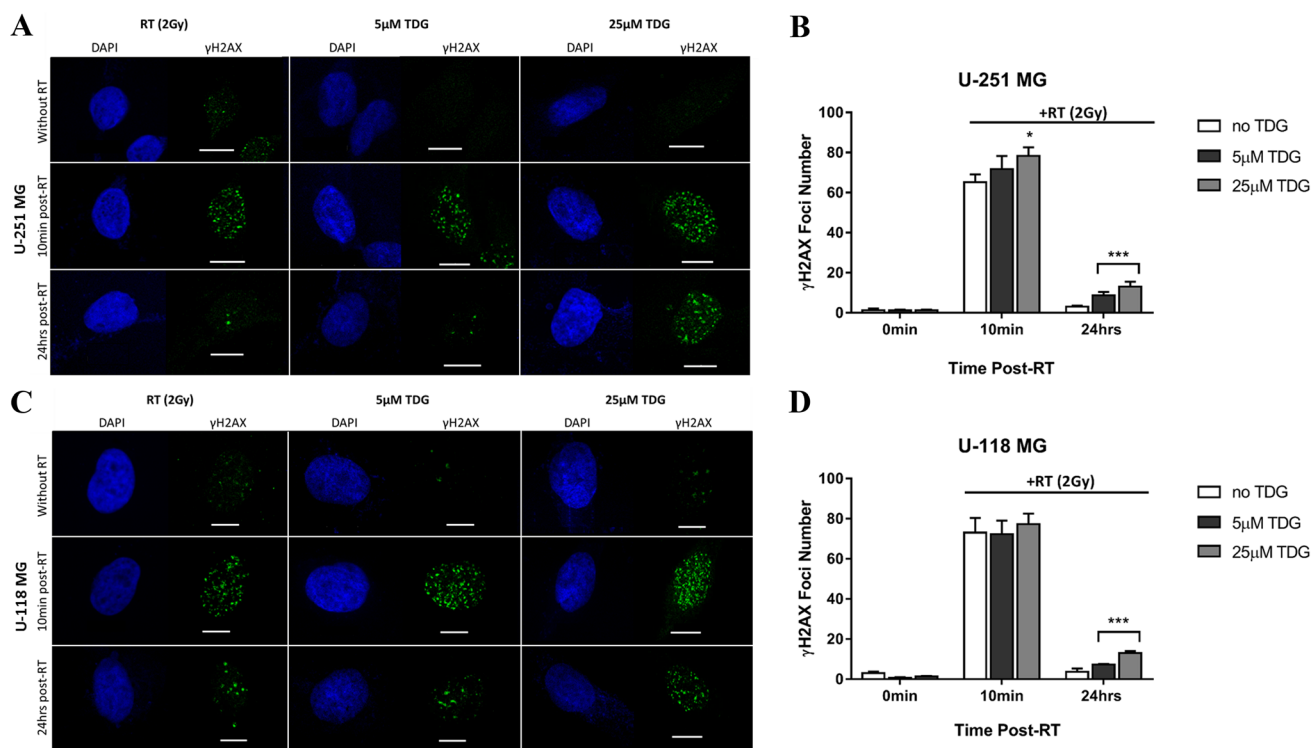


Fig. 6 Tideglusib increases the residual number radio-induced γ H2AX foci. **(a, c)** Representative images of immunofluorescence staining of γ H2AX foci. Every green dot represents the number of DSBs induced by both treatments in U-251 MG and U-118 MG glioblastoma cell lines. Magnification=100x; Scale bar=10 μ m. **(b, d)** Quantitative representation of counted foci under the confocal microscope. The number of γ H2AX foci at each condition represents the average foci number of thirty nuclei. 0 min includes the untreated condition (without TDG nor RT), and the cells treated with

5- or 25- μ M TDG (without RT). 10 min and 24 h represent the time points assessed post-radiation of cells treated with RT only (no TDG) or TDG+RT. Two-way ANOVA was done followed by a Bonferroni multiple comparison test while a one-way ANOVA with Bonferroni correction was done to assess the data at 24 h. Results are expressed as the average number of foci counted in every condition. Data represent an average of three independent experiments and are expressed as mean \pm SEM. (* $p < 0.05$; *** $p < 0.001$)

ZEN software (Fig. 7). Analysis of the number and size of the spheres included the sphere-forming unit (SFU) and the average area of spheres. The SFU of both cell lines decreased significantly when treated with TDG (Fig. 7a), was dose dependent and more prominent than RT alone (Fig. 7b). However, the most noticeable effect on sphere count was observed upon the combination of both treatments (Fig. 7c). Likewise, the combinatorial effect of TDG and RT was able to drastically reduce the size of both U-251 MG and U-118 MG spheres even at the lowest concentration of 0.1 μ M, while the concentration of 5 μ M TDG when combined with RT was able to diminish most spheres (data not shown on the figure). So, we chose not to use 5 μ M TDG in the combination experiments in 3D since we cannot perform the analyses of SFU on spheres with a size $< 40 \mu$ m. This is due to the fact that the diameter limit for a spheroid to be considered as such was 40 μ m, as described by Sart et al. [36]. For instance, if we take U-251 MG cell line when treated with a concentration of

0.1 μ M TDG, the mean of the SFU was 3.71% (SD = 0.07; SEM = 0.04) ($p = 0.00168$; $F_{4,10} = 128.6215$), and when irradiated with 2 Gy, the mean was 3.03% (SD = 0.32909; SEM = 0.19) ($p = 0.0233$; $t = 3.57$; DF = 4). However, when treated with the combination of both TDG + RT, the mean significantly decreased to 2.58% (SD = 0.190526; SEM = 0.11) ($p = 0.0048$; $F_{2,6} = 29.74693$). A similar pattern was followed by the sphere sizes (area) of both cell lines. It is noteworthy mentioning that a robust inhibitory effect of TDG on GSCs formation was noted at a much lower concentration of the drug as compared to 2D cultures. This could be explained by the notion that growing cells in 2D monolayers differs from growing them in 3D as GSCs using the sphere-formation assay. The latter allows the formation of GBM spheres with self-renewing properties in a 3D culture matrix that resembles the native microenvironment. Henceforth, different concentrations of drugs might instigate differential effects between 2 and 3D cultures, as demonstrated in our study.

Discussion

Glioblastoma multiforme (GBM), stage IV astrocytoma, represents one of the most aggressive, malignant, and infiltrative primary brain tumors [37, 38]. Treatment plans for GBM include maximal surgical resection of the infiltrated tissue followed by radiation and/or chemotherapy. However, despite all efforts made, life expectancy does not exceed a couple of months due to the poorly defined target volume during surgical procedures and to the high resistance and recurrence rates of GBM [39]. The low efficiency of available treatments in providing a better prognosis is mainly attributed to the presence of cancer stem cell (CSC) population within the tumor bulk, known as glioblastoma cancer stem-like cells (GSCs) [37]. GSCs are slowly dividing cells with the unique ability to self-renew and differentiate into various cell lineages [14], allowing them to escape conventional treatments, generate multi-drug resistant cancer cells, and reconstitute a more aggressive tumor [14, 40]. Thus, it is necessary to develop novel therapies that are able to target those GSCs and enhance the effect of conventional treatments, as it has been well acknowledged that combinatorial approaches might be more efficient in treating adult brain tumors [37].

The progression of different types of tumors and the maintenance of stem-like properties have been linked to alterations in distinct cellular signaling pathways including Notch, Sonic hedgehog (SHH), Wnt/ β -catenin pathways and p53 [14, 41]. To maintain the activation of these pathways and others, several key molecules are implicated, including GSK-3 β [42, 43]. However, the role of GSK-3 β in tumorigenesis and cancer progression is still debatable, since it functions as a tumor suppressor in some cancers while promoting growth in others [43, 44]. In glioma, GSK-3 β acts as a tumor promoter and is responsible for increased invasion and decreased apoptosis, in addition to the radio- and chemotherapy resistance [45]. In fact, studies have shown that inhibiting GSK-3 β in glioma increased the expression of apoptosis-related molecules through the increased activity of c-MYC while also decreasing pro-survival signals via the inhibition of NF- κ B [46]. A recent study revealed that knock-down of GSK-3 β in a glioma cell line promoted apoptosis and induced cytotoxicity [20]. Interestingly, this molecule has been implicated in the pathogenesis of several CNS diseases including Alzheimer's disease, Parkinson's disease, progressive supranuclear palsy, and non-insulin-dependent diabetes mellitus [43]. Tideglusib (TDG), a drug currently in Phase II clinical trials for Alzheimer's disease and progressive supranuclear palsy and showing minimal adverse effects, is a non-ATP competitive GSK-3 β inhibitor [25, 47]. Therefore, we thought of using TDG as a potential

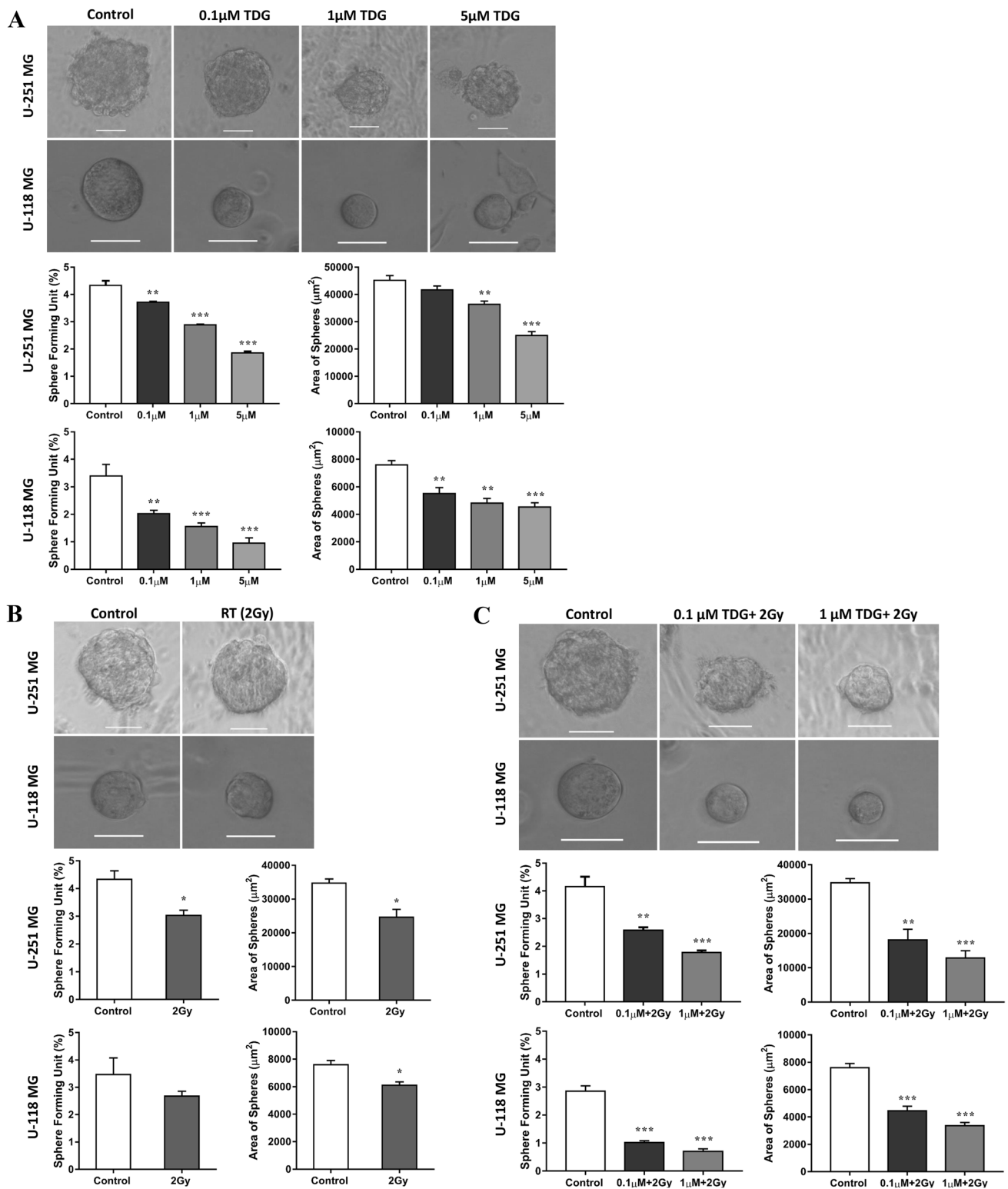
therapeutic target against GSCs and to combine this drug with radiotherapy, the first line of treatment in GBM after surgery, in an attempt to study the efficiency of this combination in targeting GSCs population.

Our study showed that TDG was able to significantly inhibit cell proliferation and viability in a time- and dose-dependent manner in two GBM cell lines, U-251 MG and U-118 MG. In addition, TDG was also able to inhibit cell migration in both cell lines, suggesting that GSK-3 β may play a key role in the invasiveness of GBM tumors, hence its inhibition as an adjunct to radiotherapy and/or chemotherapy could further halt disease progression and spreading to intact brain tissue. To further validate our results, we showed that the protein level of phosphorylated GSK-3 β increased after treatment with TDG, confirming its inhibition. So far, our findings are in agreement with the results from the previously published studies concerning other CNS tumors which have shown that TDG was able to inhibit GSK-3 β and induce apoptosis in neuroblastoma cell lines SH-SY5Y, SK-N-SH [48] and in IMR32, via the generation of reactive oxygen species (ROS) [26].

After assessing the ability of TDG in suppressing the tumorigenic properties of the GBM cell lines mentioned above, we sought to determine the effect of a combinatorial treatment of TDG with radiation on GSCs in order to assess whether TDG could ameliorate the response of cancer cells to radiation and, hence, provide a better therapeutic outcome. We performed clonogenic assay in order to track and compare the long-term effect of the two treatment modalities when applied alone and in combination on U-251 MG cells. Our results indicated that the colony-formation of U-251 MG decreased the most when cells were treated with the combination of TDG and RT as compared to when treated with each one alone.

Knowing that the most dangerous and lethal type of DNA damage induced by radiation are double-strand breaks (DSBs) [49], we performed immunofluorescent staining of γ H2AX in order to quantify the damage caused by radiation, TDG and the combinatorial treatment on both GBM cell lines. Results showed that radio-induced DSBs were almost repaired 24 h after irradiation (IR) which is in accordance with the literature [49]. Treatment with TDG alone did not induce DNA DSBs; however, it was able to sensitize both cell lines to radiation by increasing the number of unrepaired DSBs residing 24 h post-IR. Such breaks were indicated by the increased number of residual γ H2AX at that time point. According to the previous studies, the number of residual γ H2AX foci is directly related to cell death and, therefore, determines the fate of these cells [49–51].

Finally, we studied the effect of TDG and RT on the sub-population of GSCs in U-251 MG and U-118 MG cell lines using the 3D spheres culture assay with MatrigelTM in vitro [52, 53]. Our results showed that TDG inhibited the



sphere-forming ability of both cell lines and decreased the size of the formed spheres in a dose-dependent manner, while radiation had a mild effect on both mentioned characteristics. Moreover, upon combination of the two treatments, the efficiency of radiation on targeting GSCs increased significantly,

even at a very low dose of TDG (0.1 μM). Based on this experiment, we demonstrated that TDG was effective in targeting the GSC population and that its effect on the sphere-forming ability of the cells was increased by five folds while that on sphere size by 50 folds upon combination with radiation.

Fig. 7 Effect of TDG on the sphere-forming ability and sizes of human glioblastoma cell lines. **a** Representative bright-field images of G1 spheres with or without increasing concentrations of TDG treatment (**a**), RT (2 Gy) **b** and the combination of both (**c**). Images were visualized by Axiovert inverted microscope and analyzed by Carl Zeiss Zen 2012 image software. Magnification=20x; Scale bar=50 μm . Mature spheres of U-251 MG and U-118 MG were counted at day 9 and day 7, respectively, then analyzed and the sphere-forming unit (SFU) of each cell line was calculated for all conditions using the formula: $\text{SFU} = (\text{number of spheres counted} / \text{number of cells seeded}) \times 100$. The average size of 30 spheres was analyzed using ZEN software and the area of spheres was calculated accordingly (μm^2). Both the SFU and the sphere area decreased most efficiently after combining RT with TDG. One-way ANOVA and *t*-test were done to analyze the different treatment conditions. Results are represented as mean \pm SEM (* $p < 0.05$; ** $p < 0.01$; *** $p < 0.001$)

Thus, using a smaller concentration of TDG, we were able to target GSCs more efficiently than radiotherapy alone, and by combining both treatments, the properties of GSCs decreased drastically.

Despite the fact that our study is the first to show the effect of TDG combined with radiation therapy on the highly resistant GSCs, we believe that it holds several limitations. Therefore, future experiments must follow to study the effect of TDG on more GBM cell lines in vitro and experiments in vivo must be conducted as well. More specifically, we acknowledge that it is of utmost importance to assess the combined effect of TDG and radiation therapy using MTT, trypan blue, GSK expression, and wound healing assays among other experiments at a functional level. In addition, since the mechanism of action of inhibited GSK-3 β in GBM is still unknown, it is important to conduct experiments at the molecular level to determine the interaction between this kinase and the pathways affected by its inhibition and the ones involved in targeting the GSCs. We also acknowledge that it would be interesting to assess GSC origin using GBM molecular CSC markers in subsequent future studies. Yet, as a principle of proof, we believe that performing the sphere-formation assay serves as a functional assay to enrich for cells with stem-like progenitor characteristics; therefore, only cells with such potential will form spheres in 3D. Moreover, it would be very interesting to further investigate the role of TDG in inducing more damage upon its combination with RT, at the molecular level, by studying repair proteins such as pATM (phosphorylated ataxia telangiectasia mutated), KU86, KU70, XRCC4 (X-ray repair cross-complementing protein 4) and others. Based on future experiments, our data might hold a great promise for a potential treatment of GBM.

Conclusion

Although the exact mechanism of GSK3- β in glioma is still unknown, we were able to prove that inhibiting this kinase with TDG, a non-ATP competitive GSK-3 β inhibitor, might generate a novel therapeutic model for targeting glioma cells and more precisely the GSCs. We concluded also that the combination of TDG, even at low doses, with a conventional treatment might serve as a new strategy to optimize the effect of radiation on GBM.

Acknowledgments We would like to thank all members in the Abou-Kheir's Laboratory (The WAK Lab) for their help on this work. In addition, we would like to thank members of the core facilities in the DTS Building at the American University of Beirut (AUB) for their help and support.

Author contributions (CRediT author statement) JBG: Formal analysis, Investigation, Methodology, Writing- Original draft preparation. SA: Formal analysis, Investigation, Methodology, Writing—Original draft preparation. HFB: Project administration, Supervision, Formal analysis, Investigation, Methodology, Writing- Reviewing and Editing. HK: Investigation, Methodology, Writing- Reviewing and Editing. TA: Investigation, Methodology, Writing- Reviewing and Editing. RMC: Investigation, Methodology, Writing- Reviewing and Editing, Validation. FB: Investigation, Methodology, Writing- Reviewing and Editing. HH: Resources, Funding acquisition, Writing—Reviewing and Editing, Supervision, Validation, Visualization. YF: Project administration, Funding acquisition, Writing- Reviewing and Editing, Supervision, Validation, Visualization. WAK: Conceptualization, Project administration, Resources, Software, Supervision, Funding acquisition, Writing—Reviewing and Editing, Validation, Visualization.

Funding This work was supported by the Lebanese National Council for Scientific Research Grant Research Program (LNCSR-GRP) (Grant # 01-10-17; to YF), the Neuroscience Research Center, Faculty of Medicine, Lebanese University (LU) (to HH), and the Medical Practice Plan (MPP) at the American University of Beirut – Faculty of Medicine (AUB-FM) (to WAK). Funders had no role in the study design; in the collection, analysis, and interpretation of data; in the writing of the report; and in the decision to submit the article for publication.

Availability of data and material (data transparency) All data generated or analyzed during this study were included in this published article.

Compliance with ethical standards

Conflict of interest The authors declare that they have no conflict of interest.

References


- Ostrom QT, Gittleman H, Liao P, Rouse C, Chen Y, Dowling J, et al. CBTRUS statistical report: primary brain and central nervous system tumors diagnosed in the United States in 2007–2011. *Neuro-oncology*. 2014;16(Suppl 4):iv1-63.

2. Touat M, Idbaih A, Sanson M, Ligon KL. Glioblastoma targeted therapy: updated approaches from recent biological insights. *Ann Oncol*. 2017;28:1457–72.
3. Stupp R, Mason WP, van den Bent MJ, Weller M, Fisher B, Taphoorn MJ, et al. Radiotherapy plus concomitant and adjuvant temozolomide for glioblastoma. *N Engl J Med*. 2005;352:987–96.
4. AANS. Brain Tumors. Types of Brain Tumors 2019
5. Dhermain F. Radiotherapy of high-grade gliomas: current standards and new concepts, innovations in imaging and radiotherapy, and new therapeutic approaches. *Chin J Cancer*. 2014;33:16–24.
6. Yao KC, Komata T, Kondo Y, Kanzawa T, Kondo S, Germano IM. Molecular response of human glioblastoma multiforme cells to ionizing radiation: cell cycle arrest, modulation of the expression of cyclin-dependent kinase inhibitors, and autophagy. *J Neurosurg*. 2003;98:378–84.
7. Miyashita K, Kawakami K, Nakada M, Mai W, Shakoori A, Fujisawa H, et al. Potential therapeutic effect of glycogen synthase kinase 3beta inhibition against human glioblastoma. *Clin Cancer Res*. 2009;15:887–97.
8. Stupp R, Hegi ME, Mason WP, van den Bent MJ, Taphoorn MJ, Janzer RC, et al. Effects of radiotherapy with concomitant and adjuvant temozolomide versus radiotherapy alone on survival in glioblastoma in a randomised phase III study: 5-year analysis of the EORTC-NCIC trial. *Lancet Oncol*. 2009;10:459–66.
9. Stupp R, Dietrich PY, Ostermann Kraljevic S, Pica A, Maillard I, Maeder P, et al. Promising survival for patients with newly diagnosed glioblastoma multiforme treated with concomitant radiation plus temozolomide followed by adjuvant temozolomide. *J Clin Oncol*. 2002;20:1375–82.
10. Nam JY, de Groot JF. Treatment of glioblastoma. *J Oncol Pract*. 2017;13:629–38.
11. Xu HS, Qin XL, Zong HL, He XG, Cao L. Cancer stem cell markers in glioblastoma - an update. *Eur Rev Med Pharmacol Sci*. 2017;21:3207–11.
12. Singh SK, Clarke ID, Hide T, Dirks PB. Cancer stem cells in nervous system tumors. *Oncogene*. 2004;23:7267–73.
13. Gimple RC, Bhargava S, Dixit D, Rich JN. Glioblastoma stem cells: lessons from the tumor hierarchy in a lethal cancer. *Genes Dev*. 2019;33:591–609.
14. Yi Y, Hsieh IY, Huang X, Li J, Zhao W. Glioblastoma stem-like cells: characteristics, microenvironment, and therapy. *Front Pharmacol*. 2016;7:477.
15. Mittal S, Pradhan S, Srivastava T. Recent advances in targeted therapy for glioblastoma. *Expert Rev Neurother*. 2015;15:935–46.
16. Jalili-Nik M, Sadeghi MM, Mohtashami E, Mollazadeh H, Afshari AR, Sahebkar A. Zerumbone promotes cytotoxicity in human malignant glioblastoma cells through reactive oxygen species (ROS) generation. *Oxid Med Cell Longev*. 2020;2020:3237983.
17. Soukhtanloo M, Mohtashami E, Maghrouni A, Mollazadeh H, Mousavi SH, Roshan MK, et al. Natural products as promising targets in glioblastoma multiforme: a focus on NF- κ B signaling pathway. *Pharmacol Rep*. 2020;72:285–95.
18. Jope RS, Johnson GV. The glamour and gloom of glycogen synthase kinase-3. *Trends Biochem Sci*. 2004;29:95–102.
19. Jope RS, Yuskaitis CJ, Beurel E. Glycogen synthase kinase-3 (GSK3): inflammation, diseases, and therapeutics. *Neurochem Res*. 2007;32:577–95.
20. Vashishtha V, Jinghan N. Antagonistic role of GSK3 isoforms in glioma survival. *J Cancer*. 2018;9:1846–55.
21. ALZFORUM. Therapeutics-Tideglusib. ALZFORUM; 2019.
22. Lovestone S, Boada M, Dubois B, Hull M, Rinne JO, Hupertz HJ, et al. A phase II trial of tideglusib in Alzheimer's disease. *J Alzheimer's Dis*. 2015;45:75–88.
23. Tolosa E, Litvan I, Hoglinger GU, Burn D, Lees A, Andres MV, et al. A phase 2 trial of the GSK-3 inhibitor tideglusib in progressive supranuclear palsy. *Mov Disord*. 2014;29:470–8.
24. Martinez A, Gil C, Perez DI. Glycogen synthase kinase 3 inhibitors in the next horizon for Alzheimer's disease treatment. *Int J Alzheimers Dis*. 2011;2011:280502.
25. Dominguez JM, Fuertes A, Orozco L, del Monte-Millan M, Delgado E, Medina M. Evidence for irreversible inhibition of glycogen synthase kinase-3beta by tideglusib. *J Biol Chem*. 2012;287:893–904.
26. Mathuram TL, Ravikumar V, Reece LM, Karthik S, Sasikumar CS, Cherian KM. Tideglusib induces apoptosis in human neuroblastoma IMR32 cells, provoking sub-G0/G1 accumulation and ROS generation. *Environ Toxicol Pharmacol*. 2016;46:194–205.
27. Mathuram TL, Ravikumar V, Reece LM, Sasikumar CS, Cherian KM. Correlative studies unravelling the possible mechanism of cell death in tideglusib-treated human ovarian teratocarcinoma-derived PA-1 cells. *J Environm Pathol Toxicol Oncol*. 2017;36:321–44.
28. Sun A, Li C, Chen R, Huang Y, Chen Q, Cui X, et al. GSK-3beta controls autophagy by modulating LKB1-AMPK pathway in prostate cancer cells. *Prostate*. 2016;76:172–83.
29. Westermarck B. The deficient density-dependent growth control of human malignant glioma cells and virus-transformed glia-like cells in culture. *Int J Cancer*. 1973;12:438–51.
30. Macintyre EH, Pontén J, Vatter AE. The ultrastructure of human and murine astrocytes and of human fibroblasts in culture. *Acta pathologica et microbiologica Scandinavica Section A Pathol*. 1972;80:267–83.
31. van Meerloo J, Kaspers GJ, Cloos J. Cell sensitivity assays: the MTT assay. *Methods Molecular Biol (Clifton, NJ)*. 2011;731:237–45.
32. Mosmann T. Rapid colorimetric assay for cellular growth and survival: application to proliferation and cytotoxicity assays. *J Immunol Methods*. 1983;65:55–63.
33. Riss TL, Moravec RA, Niles AL, Duellman S, Benink HA, Worzella TJ, et al. Cell Viability Assays. In: Sittampalam GS, Coussens NP, Brimacombe K, Grossman A, Arkin M, Auld D, et al., (eds) *Assay Guidance Manual*. Bethesda (MD): Eli Lilly & Company and the National Center for Advancing Translational Sciences; 2004.
34. Strober W. Trypan blue exclusion test of cell viability. *Current protocols in immunology*. 2001;Appendix 3:Appendix 3B.
35. Arnold E. Quantifying cell kill and cell survival. *Basic Clin Radiobiol London 2009*. p. 41–55.
36. Sart S, Tomasi RFX, Amselem G, Baroud CN. Multiscale cytometry and regulation of 3D cell cultures on a chip. *Nature Commun*. 2017;8:469.
37. Abou-Antoun TJ, Hale JS, Lathia JD, Dombrowski SM. Brain cancer stem cells in adults and children: cell biology and therapeutic implications. *Neurotherapeutics*. 2017;14:372–84.
38. Weller M, Cloughesy T, Perry JR, Wick W. Standards of care for treatment of recurrent glioblastoma—are we there yet? *Neuro-oncology*. 2013;15:4–27.
39. Alifieris C, Trafalis DT. Glioblastoma multiforme: Pathogenesis and treatment. *Pharmacol Ther*. 2015;152:63–82.
40. Ghaffari S. Cancer, stem cells and cancer stem cells: old ideas, new developments. *F1000 Med Rep*. 2011;3:23.
41. Easton JB, Houghton PJ. mTOR and cancer therapy. *Oncogene*. 2006;25:6436–46.
42. Beurel E, Grieco SF, Jope RS. Glycogen synthase kinase-3 (GSK3): regulation, actions, and diseases. *Pharmacol Ther*. 2015;148:114–31.
43. Luo J. Glycogen synthase kinase 3beta (GSK3beta) in tumorigenesis and cancer chemotherapy. *Cancer Lett*. 2009;273:194–200.
44. Mancinelli R, Carpino G, Petrungero S, Mammola CL, Tomaipitnca L, Filippini A, et al. Multifaceted roles of GSK-3 in cancer and autophagy-related diseases. *Oxid Med Cell Longev*. 2017;2017:4629495.

45. Nakada M, MT, Pyko I, Hayashi Y, Hamada J. The Pivotal Roles of GSK3 β in Glioma Biology In: Garami M, (ed) *Molecular Targets of CNS Tumors* IntechOpen 2011.
46. Kotliarova S, Pastorino S, Kovell LC, Kotliarov Y, Song H, Zhang W, et al. Glycogen synthase kinase-3 inhibition induces glioma cell death through c-MYC, nuclear factor-kappaB, and glucose regulation. *Cancer Res.* 2008;68:6643–51.
47. del Ser T, Steinwachs KC, Gertz HJ, Andres MV, Gomez-Carrillo B, Medina M, et al. Treatment of Alzheimer's disease with the GSK-3 inhibitor tideglusib: a pilot study. *J Alzheimer's Dis.* 2013;33:205–15.
48. Bahmad HF, Chalhoub RM, Harati H, Bou-Gharios J, Assi S, Ballout F, et al. Tideglusib attenuates growth of neuroblastoma cancer stem/progenitor cells in vitro and in vivo by specifically targeting GSK-3 β . *Pharmacol Rep.* 2020. <https://doi.org/10.1007/s43440-020-00162-7>.
49. Foray N, Bourguignon M, Hamada N. Individual response to ionizing radiation. *Mutat Res.* 2016;770:369–86.
50. Mori R, Matsuya Y, Yoshii Y, Date H. Estimation of the radiation-induced DNA double-strand breaks number by considering cell cycle and absorbed dose per cell nucleus. *J Radiat Res.* 2018;59:253–60.
51. Zhao J, Guo Z, Pei S, Song L, Wang C, Ma J, et al. pATM and γ H2AX are effective radiation biomarkers in assessing the radiosensitivity of 12C6+ in human tumor cells. *Cancer Cell Int.* 2017;17:49.
52. Bahmad HF, Cheaito K, Chalhoub RM, Hadadeh O, Monzer A, Ballout F, et al. Sphere-formation assay: three-dimensional in vitro culturing of prostate cancer stem/progenitor sphere-forming cells. *Front Oncol.* 2018;8:347.
53. Mouhieddine TH, Nokkari A, Itani MM, Chamaa F, Bahmad H, Monzer A, et al. Metformin and ara-a effectively suppress brain cancer by targeting cancer stem/progenitor cells. *Front Neurosci.* 2015;9:442.

Publisher's Note Springer Nature remains neutral with regard to jurisdictional claims in published maps and institutional affiliations.

Affiliations

Jolie Bou-Gharios^{1,2} · Sahar Assi¹ · Hisham F. Bahmad^{1,3} · Hussein Kharroubi¹ · Tarek Araji¹ · Reda M. Chalhoub^{1,4} · Farah Ballout¹ · Hayat Harati² · Youssef Fares² · Wassim Abou-Kheir¹ 

¹ Department of Anatomy, Cell Biology and Physiological Sciences, Faculty of Medicine, American University of Beirut, Bliss Street, DTS Bldg, Room 116-B, Riad el Solh, PO Box 110236/41, Beirut 1107-2020, Lebanon

² Chair of Neurosurgery Department, Faculty of Medicine, Neuroscience Research Center, Lebanese University, Beirut, Lebanon

³ Present Address: Arkadi M. Rywlin M.D. Department of Pathology and Laboratory Medicine, Mount Sinai Medical Center, Miami Beach, FL, USA

⁴ Present Address: Medical Scientist Training Program, College of Medicine, Medical University of South Carolina, Charleston, SC, USA